PHYSICAL REVIEW D **88,** 024038 (2013)

Comparison of post-Newtonian templates for extreme mass ratio inspirals

Vijay Varma,[1] Ryuichi Fujita,[2] Ashok Choudhary,[3] and Bala R. Iyer[4]

[1]*Birla Institute of Technology and Science, Pilani 333031, India*

[2]*Departament de Física, Universitat de les Illes Balears, Carretera Valldemossa Kilometro 7.5, Palma de Mallorca E-07122, Spain*

[3]*Indian Institute of Science Education and Research, Pune 411008, India*

[4]*Raman Research Institute, Bangalore 560080, India*

(Received 2 May 2013; published 23 July 2013)

Extreme mass ratio inspirals (EMRIs), the inspirals of compact objects into supermassive black holes, are important gravitational wave sources for the Laser Interferometer Space Antenna (LISA). We study the performance of various post-Newtonian (PN) template families relative to the waveforms that are high-precision numerical solutions of the Teukolsky equation in the context of EMRI parameter estimation with LISA. Expressions for the time-domain waveforms TaylorT1, TaylorT2, TaylorT3, TaylorT4 and TaylorEt are derived up to 22 PN order, i.e. $\mathcal{O}(v^{44})$ (v is the characteristic velocity of the binary) beyond the Newtonian term, for a test particle in a circular orbit around a Schwarzschild black hole. The phase difference between the above 22 PN waveform families and numerical waveforms are evaluated during two-year inspirals for two prototypical EMRI systems with mass ratios 10^{-4} and 10^{-5}. We find that the dephases (in radians) for TaylorT1 and TaylorT2, respectively, are about 10^{-9} (10^{-2}) and 10^{-9} (10^{-3}) for mass ratio 10^{-4} (10^{-5}). This suggests that using 22 PN TaylorT1 or TaylorT2 waveforms for parameter estimation of EMRIs will result in accuracies comparable to numerical waveform accuracy for most of the LISA parameter space. On the other hand, from the dephase results, we find that TaylorT3, TaylorT4 and TaylorEt fare relatively poorly as one approaches the last stable orbit. This implies that, as for comparable mass binaries using the 3.5 PN phase of waveforms, the 22 PN TaylorT3 and TaylorEt approximants do not perform well enough for the EMRIs. The reason underlying the poor performance of TaylorT3, TaylorT4 and TaylorEt relative to TaylorT1 and TaylorT2 is finally examined.

DOI: 10.1103/PhysRevD.88.024038 PACS numbers: 04.25.Nx

I. INTRODUCTION

The inspiral of a stellar-mass compact object into a supermassive black hole (SMBH) is one of the most promising gravitational wave (GW) sources for space-based detectors such as eLISA.[1] The compact object typically has a mass of the order of a few solar masses, while the SMBHs detectable by eLISA are in the mass range $10^5 M_\odot$–$10^7 M_\odot$. As the mass ratio for these binaries is typically around 10^5, these systems are called extreme mass ratio inspirals (EMRIs). Gravitational waves from EMRIs can provide information about the parameters of the central black hole such as its spin, mass, and details of its stellar surroundings while also facilitating strong field tests of general relativity [1–3].

However, the gravitational wave signal is buried in a background of noise, and the signal needs to be extracted using data analysis techniques such as matched filtering. Matched filtering requires accurate templates of the gravitational waveform. For eLISA EMRI parameter estimation, the GW phase errors of the template with respect to the true signal should be less than 10 milliradians [4]. Considering eLISA is expected to detect 10–1000 EMRIs during its mission [5–7], the search for accurate waveforms for these systems is justified.

Post-Newtonian (PN) theory provides a method to predict the gravitational waveform for the early phase of inspiraling compact binaries [8]. However, since the PN approximation breaks down near the last stable orbit (LSO), numerical relativity (NR) waveforms are required beyond this point. Nevertheless, PN waveforms in the early inspiral phase are required to calibrate the NR waveforms because the computational cost for NR is very high. PN waveforms can be matched with the NR waveforms in the late inspiral and the subsequent merger and ringdown phases [9,10] to provide a cheaper alternative to using NR for the complete inspiral. PN waveforms for nonspinning comparable mass binaries in quasicircular orbits are known up to 3.5 PN order beyond the Newtonian term [11–13]. Within the post-Newtonian formalism, several nonequivalent template families such as TaylorT1, TaylorT2, TaylorT3, TaylorT4, TaylorEt and TaylorF2, among others, are possible. These 3.5 PN template families were discussed extensively in Ref. [11]. It is found that for $M < 12 M_\odot$, where M is the total mass of the binary, these 3.5 PN template families, except for TaylorT3 and TaylorEt, are equally good for the detection of gravitational waves using ground-based detectors.

The mass ratio for EMRIs is very small, 10^{-4}–10^{-7}, and one can apply black hole perturbation theory to

[1]evolved Laser Interferometer Space Antenna, also known as NGO (New Gravitational-Wave Observatory).

compute the gravitational wave emission using the mass ratio as an expansion parameter [14]. Using black hole perturbation theory, one can go to a much higher order of PN iteration for gravitational waves than for comparable masses using standard PN theory. Recently, 22 PN waveforms have been calculated for a test particle in a circular orbit around a Schwarzschild black hole [15] by solving the Teukolsky equation [16], which is a fundamental equation of the black hole perturbation theory. It is shown that the 22 PN gravitational waveforms achieve data analysis accuracies comparable to waveforms resulting from high-precision numerical solutions of the Teukolsky equation.[2] In this paper, we extend this study by calculating the different template families mentioned above up to 22 PN order using the 22 PN energy flux derived in Ref. [15]. We then investigate the performance of these Taylor approximants by evaluating the phase difference between these approximants and the waveforms that are high-precision numerical solutions of the Teukolsky equation in Refs. [22,23] over a two-year inspiral for two systems, one in the early inspiral phase and the other in the late inspiral phase of the eLISA frequency band. We find that TaylorT1 (which was also investigated in Ref. [15]) and TaylorT2 provide the best matches to numerical waveforms, while the phase difference increases by a few orders of magnitude for TaylorT3, TaylorT4 and TaylorEt. These investigations extend the results for comparable mass binaries in Ref. [11], that TaylorT3 and TaylorEt approximants are considerably different from the others and perform relatively poorly. We also discuss why the performance of TaylorT3, TaylorT4 and TaylorEt in the test particle limit becomes worse than the others. This may provide insights which should be kept in mind when one constructs new PN template families.

This paper is organized as follows: In Sec. II, we discuss the various template families along with the relevant initial conditions and calculate these approximants up to 22 PN order. In Sec. III, we evaluate the dephase between these different PN waveform approximants and a fiducial waveform that is a high-precision numerical solution of the Teukolsky equation during two-year inspirals. In Sec. IV, we summarize our main conclusions. Since the 22 PN Taylor approximants are too large to be shown in this paper, we only show them up to 4.5 PN order. The 22 PN expressions for the approximants will be publicly available online [24]. Throughout this paper, we use units $c = G = 1$.

[2]The Teukolsky equation is a first-order perturbation equation, in which the particle moves on geodesics of the black hole. Over time scales of the inverse of the mass ratio, the orbit deviates from the geodesic because of the gravitational self-force [17,18]. Using numerical results for the full relativistic first-order gravitational self-force in Ref. [19], the dephase due to the gravitational self-force is estimated as a few radians [20,21]. Thus, the gravitational self-force should be taken into account in the future.

II. THE POST-NEWTONIAN APPROXIMANTS

Post-Newtonian approximation treats the early stages of adiabatic inspiral of compact binaries as a perturbative model and expresses a binding energy, $E(v)$, and a flux, $\mathcal{F}(v)$, associated with the gravitational wave as a power series in v, where $v = (\pi MF)^{1/3}$ is the characteristic velocity, M is the total mass, and F is the gravitational wave frequency of the binary. Here, adiabatic inspiral implies that the inspiral time scale is much larger than the orbital time scale. For restricted waveforms,[3] under the adiabatic approximation, the standard energy balance equation $dE_{\rm tot}/dt = -\mathcal{F}$ gives us the following pair of coupled differential equations for the orbital phasing formula [11–13]:

$$\frac{d\phi}{dt} - \frac{v^3}{M} = 0, \tag{2.1a}$$

$$\frac{dv}{dt} + \frac{\mathcal{F}(v)}{ME'(v)} = 0. \tag{2.1b}$$

Here, $E'(v)$ is the derivative of the binding energy with respect to the characteristic velocity, v. The binding energy E is related to the total energy $E_{\rm tot}$ by $E_{\rm tot} = M(1 + E)$.

The phasing formula can also be expressed in the following equivalent parametric form, where $t_{\rm ref}$ and $\phi_{\rm ref}$ are integration constants and $v_{\rm ref}$ is an arbitrary reference velocity:

$$t(v) = t_{\rm ref} + M\int_v^{v_{\rm ref}} \frac{E'(v)}{\mathcal{F}(v)}\,dv, \tag{2.2a}$$

$$\phi(v) = \phi_{\rm ref} + \int_v^{v_{\rm ref}} v^3 \frac{E'(v)}{\mathcal{F}(v)}\,dv. \tag{2.2b}$$

Recently, the 22 PN—order energy flux for EMRIs has been calculated [15]. For the extreme mass ratio binaries, $E(v)$ is known exactly, see e.g. Ref. [25], and can be expanded and truncated to any required PN order.[4] We

[3]Restricted waveforms are obtained by retaining only the leading harmonic in the GW signal. For these waveforms the gravitational wave phase is twice the orbital phase.

[4]In contrast, for comparable mass binaries, $E(v)$ cannot be derived exactly and is computed as one of the conserved quantities associated with a specified-order PN iteration of the equation of motion. Currently, it is known up to 3 PN for nonspinning binaries in general orbits; see e.g. Ref. [8]. The flux function $F(v)$, on the other hand, is known only as a PN expansion in both the test particle and comparable mass cases, albeit to a much higher PN order in the test particle case (22 PN) relative to the comparable mass case (3.5 PN).

present, for the convenience of the reader, expressions for 4 PN $E(v)$ and 4.5 PN $\mathcal{F}(v)$ that are inputs needed to derive the 4.5 PN results displayed explicitly in later sections for brevity of presentation. In these expressions, m_1 and m_2 are the masses of the test particle and the SMBH, respectively. $M = m_1 + m_2$ is the total mass, $\nu = m_1 m_2/M^2$ is the symmetric mass ratio, and $\gamma = 0.577216\ldots$ is the Euler constant.

$$E_4(v) = -\frac{1}{2}\nu v^2\left[1 - \frac{3v^2}{4} - \frac{27v^4}{8} - \frac{675v^6}{64} - \frac{3969v^8}{128}\right], \tag{2.3}$$

$$\begin{aligned}\mathcal{F}_{4.5}(v) = \frac{32}{5}\nu^2 v^{10}\Bigg[1 &- \frac{1247v^2}{336} + 4\pi v^3 - \frac{44711v^4}{9072} - \frac{8191\pi v^5}{672} + v^6\left\{\frac{6643739519}{69854400} + \frac{16\pi^2}{3} - \frac{1712\gamma}{105} - \frac{856}{105}\log(16v^2)\right\} \\ &- \frac{16285\pi v^7}{504} + v^8\left\{-\frac{323105549467}{3178375200} - \frac{1369\pi^2}{126} + \frac{232597\gamma}{4410} + \frac{39931}{294}\log(2) - \frac{47385}{1568}\log(3) + \frac{232597}{4410}\log(v)\right\} \\ &+ \pi v^9\left\{\frac{265978667519}{745113600} - \frac{6848\gamma}{105} - \frac{3424}{105}\log(16v^2)\right\}\Bigg].\end{aligned} \tag{2.4}$$

Approximate waveforms are obtained by inserting the expressions for $E(v)$ and $\mathcal{F}(v)$ at consistent PN order into the phasing formula—these waveforms are referred to as Taylor approximants. There are several ways of inserting these expressions into the phasing formula, leading to different approximants such as TaylorT1, TaylorT4, TaylorT2, TaylorT3, TaylorEt and TaylorF2 [11]. We have calculated these approximants up to 22 PN order for the EMRI case. We shall now discuss these approximants while presenting our results up to 4.5 PN. The method for calculating the phase of the gravitational waveform is left for the next section. The complete 22 PN expressions will be available online [24].

A. TaylorT1

The TaylorT1 approximant is obtained by using the expressions for binding energy, $E(v)$, and flux, $\mathcal{F}(v)$, as they appear in Eqs. (2.3) and (2.4) in the phasing formula, Eq. (2.1), and solving the resulting equations involving the rational polynomial $\mathcal{F}(v)/E'(v)$ numerically:

$$\frac{d\phi^{(\mathrm{T1})}}{dt} - \frac{v^3}{M} = 0, \tag{2.5a}$$

$$\frac{dv}{dt} + \frac{\mathcal{F}(v)}{ME'(v)} = 0. \tag{2.5b}$$

In the above equations, $v \equiv v^{(\mathrm{T1})}$, but for simplicity we omit the superscript. The expressions for $E(v)$ and $\mathcal{F}(v)$ are to be truncated to consistent PN order to obtain the approximant of that order. This is followed for all the approximants in this section.

B. TaylorT4

TaylorT4 goes one step further than TaylorT1 by expanding the rational polynomial $\mathcal{F}(v)/E'(v)$ and truncating it to the required PN order [26]. The characteristic velocity, $v^{(\mathrm{T4})}(t) \equiv v(t)$ at 4.5 PN, is given for TaylorT4 by

$$\begin{aligned}\frac{dv}{dt} = \frac{32}{5}\frac{\nu}{M}v^9\Bigg[1 &- \frac{743v^2}{336} + 4\pi v^3 + \frac{34103v^4}{18144} - \frac{4159\pi v^5}{672} + v^6\left\{\frac{16447322263}{139708800} + \frac{16\pi^2}{3} - \frac{1712\gamma}{105} - \frac{856}{105}\log(16v^2)\right\} \\ &- \frac{4415\pi v^7}{4032} + v^8\left\{\frac{3959271176713}{25427001600} - \frac{361\pi^2}{126} + \frac{124741\gamma}{4410} + \frac{127751}{1470}\log(2) - \frac{47385}{1568}\log(3) + \frac{124741}{4410}\log(v)\right\} \\ &+ \pi v^9\left\{\frac{343801320119}{745113600} - \frac{6848\gamma}{105} - \frac{3424}{105}\log(16v^2)\right\}\Bigg].\end{aligned} \tag{2.6}$$

Similarly to TaylorT1, Eq. (2.1a) gives the evolution of the orbital phase for TaylorT4.

C. TaylorT2

TaylorT2 uses the parametric form of the phasing formula, Eq. (2.2). The ratio $E'(v)/\mathcal{F}(v)$ is expanded and truncated to the required PN order. Upon integration, we obtain the following equations for $\phi(v)$ and $t(v)$ at 4.5 PN order:

$$\phi_{4.5}^{(\mathrm{T2})}(v) = \phi_{\mathrm{ref}}^{(\mathrm{T2})} - \frac{1}{32\nu v^5}\Bigg[1 + \frac{3715v^2}{1008} - 10\pi v^3 + \frac{15293365v^4}{1016064} + \frac{38645\pi}{672}v^5\log\left(\frac{v}{v_{\mathrm{lso}}}\right) + v^6\Bigg\{\frac{12348611926451}{18776862720} - \frac{160\pi^2}{3} - \frac{1712\gamma}{21} - \frac{856}{21}\log(16v^2)\Bigg\} + \frac{77096675\pi v^7}{2032128} + v^8\Bigg\{\frac{2550713843998885153}{2214468081745920} - \frac{45245\pi^2}{756} - \frac{9203\gamma}{126} - \frac{252755}{2646}\log(2) - \frac{78975}{1568}\log(3) - \frac{9203}{126}\log(v)\Bigg\} + \pi v^9\Bigg\{-\frac{93098188434443}{150214901760} + \frac{80\pi^2}{3} + \frac{1712\gamma}{21} + \frac{856}{21}\log(16v^2)\Bigg\}\Bigg], \tag{2.7a}$$

$$t_{4.5}^{(\mathrm{T2})}(v) = t_{\mathrm{ref}}^{(\mathrm{T2})} - \frac{5M}{256\nu v^8}\Bigg[1 + \frac{743v^2}{252} - \frac{32\pi v^3}{5} + \frac{3058673v^4}{508032} - \frac{7729\pi v^5}{252} + v^6\Bigg\{-\frac{10052469856691}{23471078400} + \frac{128\pi^2}{3} + \frac{6848\gamma}{105} + \frac{3424}{105}\log(16v^2)\Bigg\} - \frac{15419335\pi v^7}{127008} + v^8\Bigg\{\Bigg(\frac{2496799162103891233}{461347517030400} - \frac{18098\pi^2}{63} - \frac{36812\gamma}{105} - \frac{202204}{441}\log(2) - \frac{47385}{196}\log(3)\Bigg)\log(v) - \frac{18406}{105}\log^2(v)\Bigg\} + \pi v^9\Bigg\{-\frac{102282756713483}{23471078400} + \frac{512\pi^2}{3} + \frac{54784\gamma}{105} + \frac{27392}{105}\log(16v^2)\Bigg\}\Bigg]. \tag{2.7b}$$

Here t_{ref} and ϕ_{ref} are integration constants. t_{ref} is fixed by setting $t = 0$ when $v = v_0$, the initial velocity.

D. TaylorT3

To get the TaylorT3 approximant, the expression for $t(v)$ generated in TaylorT2 is inverted to get $v(t)$. This is then used to obtain $\phi(t) \equiv \phi(v(t))$. TaylorT3 also gives the instantaneous gravitational wave frequency F by $F \equiv d\phi/(\pi dt) = v^3/(\pi M)$. The TaylorT3 approximant at 4.5 PN order is given by

$$\phi_{4.5}^{(\mathrm{T3})}(t) = \phi_{\mathrm{ref}}^{(\mathrm{T3})} - \frac{1}{\nu\theta^5}\Bigg[1 + \frac{3715\theta^2}{8064} - \frac{3\pi\theta^3}{4} + \frac{9275495\theta^4}{14450688} + \frac{38645\pi\theta^5}{21504}\log\left(\frac{\theta}{\theta_{\mathrm{lso}}}\right) + \theta^6\Bigg\{\frac{831032450749357}{57682522275840} - \frac{53\pi^2}{40} - \frac{107\gamma}{56} - \frac{107}{56}\log(2\theta)\Bigg\} + \frac{188516689\pi\theta^7}{173408256} + \theta^8\Bigg\{\frac{11715802333726918585}{2073248288647151616} - \frac{191257\pi^2}{387072} - \frac{312247}{451584}\log^2(2) + \frac{2446934992845948193}{188967942975651840}\log(2) - \frac{236925}{401408}\log(2)\log(3) - \frac{78975}{401408}\log(3) - \frac{\gamma(208343 + 386526\log(2))}{451584} - \frac{45245\pi^2}{64512}\log(2) + \Bigg(-\frac{2583981498376602913}{188967942975651840} + \frac{45245\pi^2}{64512} + \frac{9203\gamma}{10752} + \frac{14873}{56448}\log(2) + \frac{236925}{401408}\log(3)\Bigg)\log(\theta) + \frac{9203\log^2(\theta)}{21504}\Bigg\} + \pi\theta^9\Bigg\{\frac{587519428177201}{192275074252800} - \frac{33\pi^2}{800} - \frac{321\gamma}{1120} - \frac{321}{1120}\log(2\theta)\Bigg\}\Bigg], \tag{2.8a}$$

$$F_{4.5}^{(\mathrm{T3})}(t) = \frac{\theta^3}{8\pi M}\Bigg[1 + \frac{743\theta^2}{2688} - \frac{3\pi\theta^3}{10} + \frac{1855099\theta^4}{14450688} - \frac{7729\pi\theta^5}{21504} + \theta^6\Bigg\{-\frac{720817631400877}{288412611379200} + \frac{53\pi^2}{200} + \frac{107\gamma}{280} + \frac{107}{280}\log(2\theta)\Bigg\} - \frac{188516689\pi\theta^7}{433520640} + \theta^8\Bigg\{-\frac{2033421792006076349}{3101012397549158400} + \frac{33589\pi^2}{215040} + \frac{312247}{752640}\log^2(2) - \frac{2463531507726173473}{314946571626086400}\log(2) + \frac{142155}{401408}\log(2)\log(3) + \frac{\gamma(79501 + 386526\log(2))}{752640} + \frac{9049\pi^2}{21504}\log(2) + \Bigg(\frac{2530066816481608993}{314946571626086400} - \frac{9049\pi^2}{21504} - \frac{9203\gamma}{17920} - \frac{14873}{94080}\log(2) - \frac{142155}{401408}\log(3)\Bigg)\log(\theta) - \frac{9203}{35840}\log^2(\theta)\Bigg\} + \pi\theta^9\Bigg\{-\frac{573742575758641}{240343842816000} + \frac{33\pi^2}{1000} + \frac{321\gamma}{1400} + \frac{321}{1400}\log(2\theta)\Bigg\}\Bigg], \tag{2.8b}$$

where $\theta(t)$ is given by $\theta = [\nu(t_{\rm ref} - t)/(5M)]^{-1/8}$. Given an initial velocity v_0, one can find the initial frequency F_0 by $F_0 = v_0^3/(\pi M)$. To find $t_{\rm ref}$, one solves Eq. (2.8b) at $t = 0$ and $F = F_0$.

E. TaylorEt

TaylorEt is expressed as a power series of a new function, $\zeta = -2E/\nu$ [27]. Equation (2.3) for $E(v)$ can be expressed in terms of $x = v^2$ to get $\zeta(x)$. This is then inverted to obtain $x(\zeta)$:

$$x(\zeta) = \zeta\left[1 + \frac{3\zeta}{4} + \frac{9\zeta^2}{2} + \frac{405\zeta^3}{16} + \frac{2511\zeta^4}{16}\right]. \tag{2.9}$$

From the phasing formula Eqs. (2.1a) and (2.9), we get an expression for the evolution of phase in terms of ζ [cf. Eq. (2.11a)]. Under the new variable, ζ, Eq. (2.1b) of the phasing formula transforms to

$$\frac{d\zeta}{dt} = \frac{2\mathcal{F}(v(\zeta))}{\nu M}. \tag{2.10}$$

The TaylorEt approximant is, essentially, the gravitational wave phasing equations expressed in terms of ζ. At 4.5 PN order, it is given by

$$\frac{d\phi^{(\rm Et)}(t)}{dt} = \frac{\zeta^{3/2}}{M}\left[1 + \frac{9\zeta}{8} + \frac{891\zeta^2}{128} + \frac{41445\zeta^3}{1024} + \frac{8413875\zeta^4}{32768}\right], \tag{2.11a}$$

$$\begin{aligned}\frac{d\zeta}{dt} = \frac{64\nu\zeta^5}{5M}\Bigg[&1 + \frac{13\zeta}{336} + 4\pi\zeta^{3/2} + \frac{117857\zeta^2}{18144} + \frac{4913\pi}{672}\zeta^{5/2} + \zeta^3\left\{\frac{37999588601}{279417600} + \frac{16\pi^2}{3} - \frac{1712\gamma}{105} - \frac{856}{105}\log(16\zeta)\right\} \\ &+ \frac{129817\pi}{2304}\zeta^{7/2} + \zeta^4\left\{\frac{3677099151569}{5085400320} + \frac{2663\pi^2}{126} - \frac{198827\gamma}{4410} - \frac{87961}{1470}\log(2) - \frac{47385}{1568}\log(3)\right. \\ &\left. - \frac{198827}{8820}\log(\zeta)\right\} + \pi\zeta^{9/2}\left\{\frac{1130297606413}{1490227200} - \frac{6848\gamma}{105} - \frac{3424}{105}\log(16\zeta)\right\}\Bigg].\end{aligned} \tag{2.11b}$$

As in the case of TaylorT3, we can find F_0, given v_0. Noting that $F \equiv d\phi/(\pi dt)$, initial conditions for TaylorEt can be set up by solving Eq. (2.11a) for ζ_0 by setting the left-hand side to πF_0.

F. TaylorF2

TaylorF2 is a Fourier-domain approximant based on the stationary phase approximation (SPA). Under the SPA, the waveform in the Fourier domain is expressed as

$$\tilde{h}^{\rm spa}(f) = \frac{a(t_f)}{\sqrt{\dot{F}(t_f)}} e^{i[\psi_f(t_f) - \pi/4]}, \qquad \psi_f(t) \equiv 2\pi f t - 2\phi(t), \tag{2.12}$$

where t_f is the saddle point, defined by solving for t when $d\psi_f(t)/dt = 0$, i.e. the time t_f when the gravitational wave frequency $F(t)$ becomes equal to the Fourier variable, f. In the adiabatic approximation [where Eqs. (2.2a) and (2.2b) hold], the values of t_f and $\psi_f(t_f)$ are given by

$$t_f = t_{\rm ref} + M\int_{v_f}^{v_{\rm ref}} \frac{E'(v)}{\mathcal{F}(v)} dv, \tag{2.13a}$$

$$\psi_f(t_f) = 2\pi f t_{\rm ref} - \phi_{\rm ref} + 2\int_{v_f}^{v_{\rm ref}} (v_f^3 - v^3)\frac{E'(v)}{\mathcal{F}(v)} dv, \tag{2.13b}$$

where $v_f = (\pi M f)^{1/3}$.

Using expressions of energy and flux and expanding the ratio $E'(v)/\mathcal{F}(v)$ in Eq. (2.13) to consistent PN order leads to an expression which can be integrated explicitly, resulting in the TaylorF2 approximant. The phase of the Fourier-domain waveform up to 4.5 PN order is given by

$$\psi^{(\mathrm{F2})}_{4.5}(f) = 2\pi f t_c - \phi_c - \frac{\pi}{4} + \frac{3}{128\nu v^5}\Bigg[1 + \frac{3715v^2}{756} - 16\pi v^3 + \frac{15293365v^4}{508032} + \frac{38645\pi v^5}{252}\log\left(\frac{v}{v_{\mathrm{lso}}}\right) + v^6\left\{\frac{11583231236531}{4694215680} - \frac{640\pi^2}{3} - \frac{6848\gamma}{21} - \frac{3424}{21}\log(16v^2)\right\} + \frac{77096675\pi v^7}{254016} + v^8\left\{\left(-\frac{2550713843998885153}{276808510218240} + \frac{90490\pi^2}{189} + \frac{36812\gamma}{63} + \frac{1011020}{1323}\log(2) + \frac{78975}{196}\log(3)\right)\left(\log(v) - \frac{1}{3}\right) + \frac{18406}{63}\log^2(v)\right\} + \pi v^9\left\{\frac{105344279473163}{18776862720} - \frac{640\pi^2}{3} - \frac{13696\gamma}{21} - \frac{6848}{21}\log(16v^2)\right\}\Bigg], \tag{2.14}$$

where t_c and ϕ_c can be chosen arbitrarily and $v = (\pi M f)^{1/3}$.

The behavior of TaylorF2 has already been investigated up to 3.5 PN order for comparable mass binaries [11–13]. One must keep in mind that the stationary phase approximation, on which TaylorF2 is based, is valid only up to 4.5 PN order [28,29]. Thus, beyond 4.5 PN, the Fourier transform of the waveform has correction terms for the stationary phase approximation to the Fourier transform in Eq. (2.12). However, as a start, in this paper, we have obtained the TaylorF2 approximant up to 22 PN order by assuming Eq. (2.12) is valid even beyond 4.5 PN. Further studies, computing terms beyond the leading one [11–13], are needed to look for a good frequency-domain approximant at higher PN orders and will be investigated in the future.

III. COMPARISON WITH HIGH-PRECISION NUMERICAL SOLUTIONS OF THE TEUKOLSKY EQUATION

To investigate the behavior of different analytical PN families described in Sec. II, we calculate the phase of the gravitational wave signal during a two-year quasicircular inspiral of two systems of binaries called System I and System II as considered in Refs. [15,30–32]. We compare this phase with the phase calculated using waveforms that are high-precision numerical solutions of the Teukolsky equation; the difference between these phases is called the dephase. System I has masses $(m_1, m_2) = (10, 10^5)M_\odot$, with $m_1/m_2 = 10^{-4}$; it inspirals from $r_{\mathrm{in}} \simeq 29M$ to $r_{\mathrm{fin}} \simeq 16M$ during a two-year period, with gravitational wave frequencies in the range $f_{\mathrm{GW}} \in [4\times10^{-3}, 10^{-2}]$ Hz. System II has masses $(m_1, m_2) = (10, 10^6)M_\odot$, with $m_1/m_2 = 10^{-5}$; it inspirals from $r_{\mathrm{in}} \simeq 11M$ to $r_{\mathrm{fin}} \simeq 6M$ (LSO) during a two-year period, with gravitational wave frequencies in the range $f_{\mathrm{GW}} \in [1.8\times10^{-3}, 4.4\times10^{-3}]$ Hz. In the frequency band of eLISA, System I corresponds to the early inspiral phase of an EMRI, while System II corresponds to the late inspiral phase. Note that the phases shown in the figures of this section are gravitational wave phases which are twice the orbital phases.

Matched filtering can give signal-to-noise ratios (SNRs) of up to $\rho \sim 100$ [33,34] for the strongest EMRI signals detectable by eLISA. This means eLISA can detect phases up to an accuracy of order $1/\rho \sim 10$ milliradians [4]. Therefore, while considering the dephase results of this paper, we expect PN waveforms to have accuracies comparable to those provided by numerical waveforms if the dephase is less than 10^{-2} radians.

The numerical waveforms we use are based on those in Refs. [22,23], which solve the Teukolsky equation. The truncation of the l mode limits the accuracy of the numerical calculations. We use the same data generated for Ref. [15], which is based on $l = 25$ calculations and gives relative error better than 10^{-14} up to the LSO.

A. Dephase between TaylorT1 and numerical results

The dephase between TaylorT1 and numerical waveforms (cf. Fig. 1) was shown in Ref. [15]. We present the results here for comparison.[5] For System I (II), the absolute values of the dephasing between the TaylorT1 waveforms and the numerical waveforms after the two-year inspiral are about $7\times10^{1}(8\times10^{3})$, $7\times10^{-3}(8)$, $7\times10^{-6}(5\times10^{-1})$, $8\times10^{-9}(3\times10^{-2})$ and $10^{-9}(5\times10^{-3})$ radians for 5.5 PN, 10 PN, 14 PN, 18 PN and 22 PN, respectively. It is also suggested in Ref. [15] that using 22 PN TaylorT1 waveforms for EMRIs will result in accuracy of data analysis comparable to that resulting from high-precision numerical waveforms, as the dephase is less than 10^{-2} radians for most of the parameter space of eLISA. We also note that 10 PN TaylorT1 waveforms may be comparable in accuracy of data analysis to numerical waveforms for System I.

We now extend this study by investigating the behavior of other PN Taylor families by evaluating their dephases during the same inspiral.

B. Dephase between TaylorT4 and numerical results

The calculation of the phase of TaylorT4 is very similar to that of TaylorT1 and numerical waveforms. We use the relation

$$\phi(t) = \int_0^t (d\phi/dt')dt' = \int_{v_0}^{v(t)} \frac{(d\phi/dt')}{(dv'/dt')}dv'. \tag{3.1}$$

[5]Figure 1 is slightly different from the dephase results of Ref. [15]. This is because in Ref. [15] the TaylorT1 phase was calculated without expanding dE/dv in v.

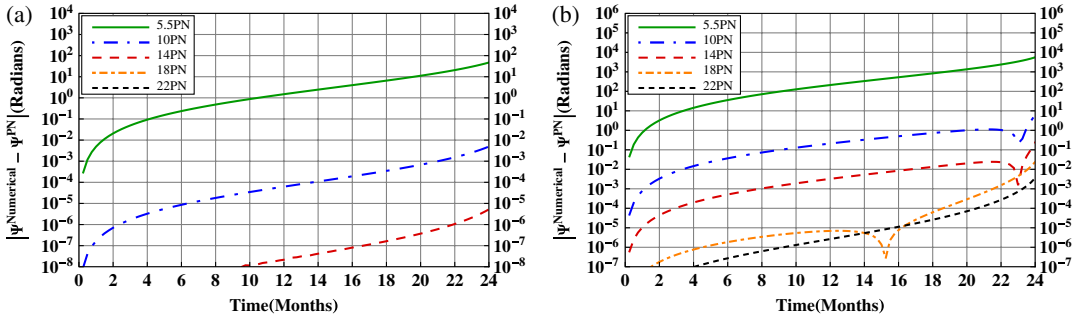

FIG. 1 (color online). Absolute value of the dephase between TaylorT1 PN waveforms and numerical waveforms during two-year inspirals as a function of time in months. The left panel shows the dephase for System I having masses $(m_1, m_2) = (10, 10^5)M_\odot$ for $r_{\rm in} \simeq 29M$ to $r_{\rm fin} \simeq 16M$ sweeping GW frequencies in the range $f_{\rm GW} \in [4 \times 10^{-3}, 10^{-2}]$ Hz. The right panel shows the dephase for System II having masses $(m_1, m_2) = (10, 10^6)M_\odot$ for $r_{\rm in} \simeq 11M$ to $r_{\rm fin} \simeq 6M$ (LSO) sweeping GW frequencies in the range $f_{\rm GW} \in [1.8 \times 10^{-3}, 4.4 \times 10^{-3}]$ Hz. System I (System II) corresponds to the early (late) inspiral phase of the eLISA frequency band. Note that the dephase between 18 PN (22 PN) TaylorT1 waveforms and numerical waveforms at the end of the two-year inspiral for System I is about 8×10^{-9} (10^{-9}) radians, which falls below the lowest value of dephase in the left panel. (a) System-I for TaylorT1. (b) System-II for TaylorT1.

Here, $d\phi/dt$ is given by Eq. (2.1a), v_0 is the velocity at the starting of the two-year inspiral, and $v(t)$ can be obtained by solving the equation $t - \int_{v_0}^{v(t)} 1/(dv/dt)dv = 0$ for a given time t. For TaylorT4, dv/dt is given by Eq. (2.6), while for numerical waveforms, dv/dt is obtained from the solution of Teukolsky equation [15,22,23].

The dephase results are shown in Figs. 2(a) and 2(b). For System I (II), the absolute values of the dephasing between the TaylorT4 waveforms and the numerical waveforms after the two-year inspiral are about $2 \times 10^2 (3 \times 10^4)$, $7 \times 10^{-1} (7 \times 10^3)$, $6 \times 10^{-3} (2 \times 10^3)$, $5 \times 10^{-5} (8 \times 10^2)$ and $5 \times 10^{-7} (3 \times 10^2)$ radians for 5.5 PN, 10 PN, 14 PN, 18 PN and 22 PN, respectively. This suggests that 14 PN or higher-order TaylorT4 waveforms are comparable in accuracy of data analysis to numerical waveforms for the early inspiral phase (System I), but the accuracy is low for the late inspiral phase (System II), particularly, near the LSO.

By comparing with Fig. 1, we see that the dephase for TaylorT4 is a few orders of magnitude worse than that for TaylorT1. This can be explained as follows: In the test particle limit, dE/dv, given by

$$\frac{dE}{dv} = -v \frac{(1 - 6v^2)}{(1 - 3v^2)^{3/2}}, \tag{3.2}$$

goes to zero as one approaches the LSO at $v = 1/\sqrt{6}$. Therefore, the series expansion of $(dE/dv)^{-1}$ converges very slowly around the LSO. Noting that TaylorT1 and TaylorT4 differ in whether or not the series expansion of $(dE/dv)^{-1}$ is performed in obtaining dv/dt, one can expect that TaylorT1 will be more accurate than TaylorT4 near the LSO. This suggests that factorization to avoid a pole at the LSO leads to improvement in the accuracy of dv/dt. We note that in Refs. [35,36], factorization is performed for the energy flux, $\mathcal{F}(v)$, to deal with a pole at the light ring, $v = 1/\sqrt{3}$. Thus, one may also have to factorize the pole at the light ring when considering the case beyond the LSO.

C. Dephase between TaylorT2 and numerical results

TaylorT2 expresses the orbital phase, $\phi(v)$, and the time, $t(v)$, as functions of v. For a given time T, we solve the equation $T - t(v) = 0$ to get the velocity, $v(T)$. Given the velocity, one can compute the phase as

$$\phi(t) = \phi(v(t)). \tag{3.3}$$

$\phi_{\rm ref}$ in Eq. (2.7a) is chosen such that $\phi(t = 0) = 0$.

The dephase results are shown in Figs. 2(c) and 2(d). For System I (II), the absolute values of the dephasing between the TaylorT2 waveforms and the numerical waveforms after the two-year inspiral are about $9 \times 10^1 (10^4)$, $4 \times 10^{-2} (6 \times 10^2)$, $5 \times 10^{-6} (5)$, $5 \times 10^{-9} (10^{-2})$ and $10^{-9} (8 \times 10^{-4})$ radians for 5.5 PN, 10 PN, 14 PN, 18 PN and 22 PN, respectively. Therefore, for TaylorT2, 10 PN (18 PN) waveforms may provide accuracies comparable to those provided by numerical waveforms for System I (System II).

As can be seen by comparing with Fig. 1, the dephase of TaylorT2 is comparable or lesser than TaylorT1 during the inspirals. However, one needs to keep in mind that for calculating the phase from the TaylorT2 approximant, a pair of transcendental equations needs to be solved, which can be very time consuming and expensive.

D. Dephase between TaylorEt and numerical results

TaylorEt expresses $d\phi/dt$ and $d\zeta/dt$ as power-series expansions of $\zeta = -2E/\nu$. For a given time T, we solve the equation $T - \int_{\zeta_0}^{\zeta(T)} 1/(d\zeta/dt)d\zeta = 0$ to get $\zeta(T)$, where ζ_0 and $\zeta(T)$ are the values of ζ at $t = 0$ and time T, respectively.

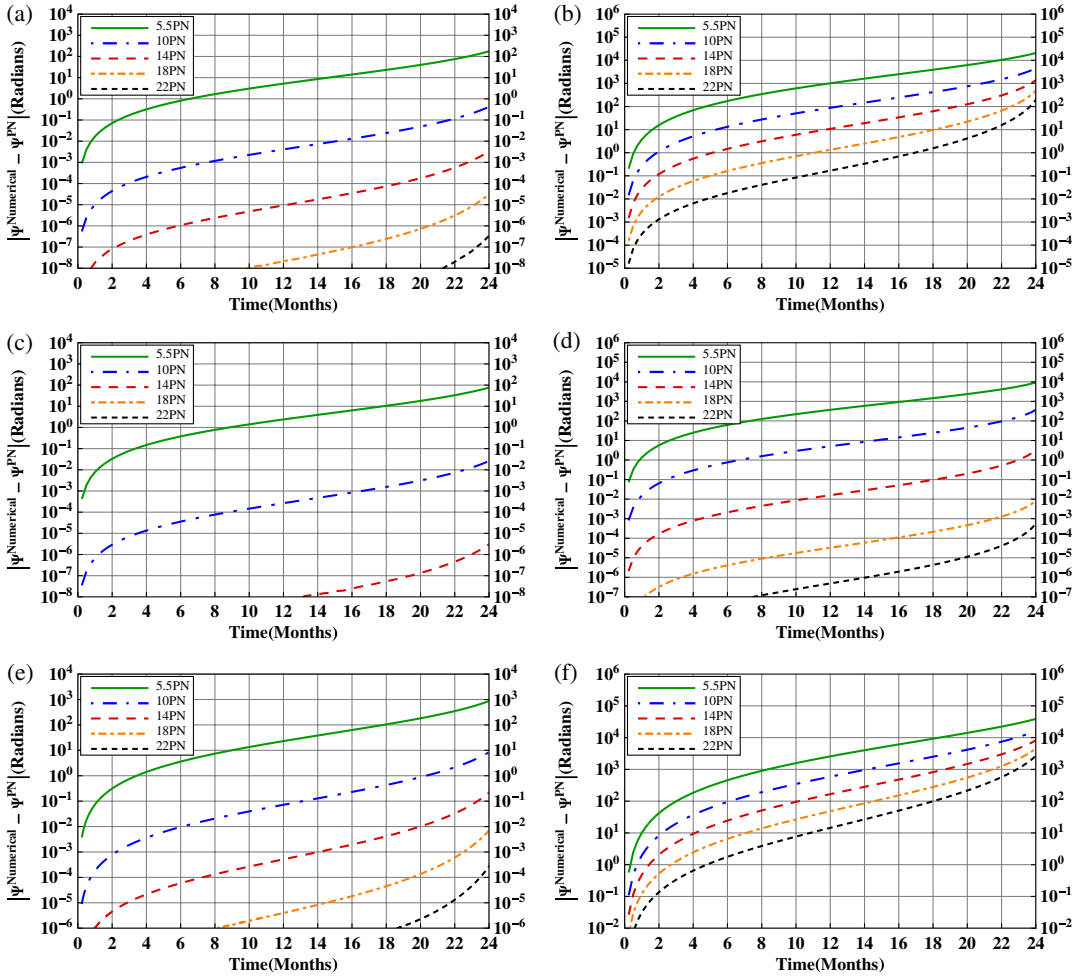

FIG. 2 (color online). Absolute value of the dephase between different PN waveforms and numerical waveforms during two-year inspirals as a function of time in months. The left (right) panel shows the dephase for System I (System II). Note that the dephase between 18 PN (22 PN) TaylorT2 waveforms and numerical waveforms at the end of the two-year inspiral for System I is about 5×10^{-9} (10^{-9}) radians, which falls below the lowest value of dephase shown in (c). If the dephase is less than 10 milliradians, the PN waveforms will provide data analysis accuracies comparable to those provided by the numerical waveforms. Therefore, we expect that 18 PN waveforms for TaylorT2 are comparable in accuracy of data analysis to numerical waveforms for most of the EMRI parameter space of eLISA. 14 PN and 18 PN waveforms are required for TaylorT4 and TaylorEt, respectively, to be comparable to numerical waveforms even in the early inspiral phase (System I). The accuracy of TaylorT4 and TaylorEt for System II (which goes up to the LSO) is not comparable to numerical waveform accuracy. (a) System-I for TaylorT4. (b) System-II for TaylorT4. (c) System-I for TaylorT2. (d) System-II for TaylorT2. (e) System-I for TaylorEt. (f) System-II for TaylorEt.

The phase can now be evaluated as

$$\phi(t) = \int_0^t (d\phi/dt')dt' = \int_{\zeta_0}^{\zeta(t)} \frac{(d\phi/dt')}{(d\zeta/dt')} d\zeta, \qquad (3.4)$$

where $(d\phi/dt')$ and $(d\zeta/dt')$ are given in Eq. (2.11).

The dephase results are shown in Figs. 2(e) and 2(f). For System I (II), the absolute values of the dephasing between the TaylorEt waveforms and the numerical waveforms after the two-year inspiral are about $10^3(6 \times 10^4)$, $9(2 \times 10^4)$, $3 \times 10^{-1}(9 \times 10^3)$, $8 \times 10^{-3}(7 \times 10^3)$ and $4 \times 10^{-4}(4 \times 10^3)$ radians for 5.5 PN, 10 PN, 14 PN, 18 PN and 22 PN, respectively. This suggests that 18 PN and 22 PN TaylorEt waveforms are comparable in accuracy of data analysis to numerical waveforms for the early inspiral phase (System I) of the eLISA frequency band, but the accuracy is low for the late inspiral phase (System II).

As in the case of TaylorT4 in Sec. III B, the reason that the performance of TaylorEt is much worse than that of TaylorT1 can be related to the poor convergence of the series expansion of $(dE/dv)^{-1}$ or dv/dt around the LSO. Solving $\zeta = -2E/\nu$ iteratively,[6] the new variable ζ in

[6]One can solve $\zeta = -2E/\nu$ to obtain the explicit expression for $v(\zeta)$ without performing a series expansion in terms of v. But the explicit expression for $v(\zeta)$ may not be useful to implement, since it contains the square root of polynomial functions of ζ.

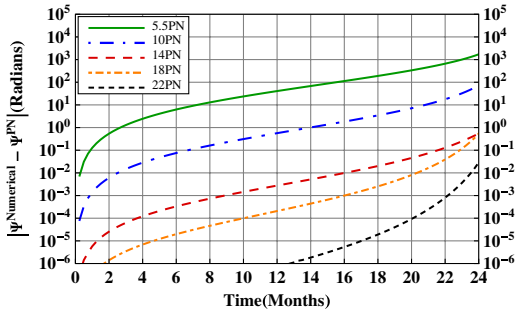

FIG. 3 (color online). Absolute value of the dephase between TaylorT3 PN waveforms and numerical waveforms during two-year inspirals for System I as a function of time in months. TaylorT3 is found to behave poorly for System II as it goes up to the last stable orbit (LSO). We expect that 22 PN TaylorT3 waveforms are required to get data analysis accuracies comparable to those provided by numerical waveforms for System I.

TaylorEt can be related to v as in Eq. (2.9). One can also derive the same relation using $v(\zeta) = \int (d\zeta'/dv)^{-1} d\zeta'$. Noting $(d\zeta/dv)^{-1} = -\nu(dE/dv)^{-1}/2$, we see that the integrand of $v(\zeta)$ contains a pole at the LSO. Then, one may expect that v as a series expansion in terms of ζ does not converge very well around the LSO. Hence, functions of ζ in TaylorEt, which are computed by using a series expansion of $v(\zeta)$, will not converge well.

E. Dephase between TaylorT3 and numerical results

TaylorT3 gives the orbital phase, $\phi(t)$, and the instantaneous gravitational wave frequency, $F(t)$, as functions of $\theta(t)$, which is a function of time. For any given time t, we can find the phase as

$$\phi(t) = \phi(\theta(t)). \tag{3.5}$$

As in TaylorT2, $\phi_{\rm ref}$ is chosen such that $\phi(t = 0) = 0$.

The dephase results for System I are shown in Fig. 3. For System I, the absolute values of the dephasing between the TaylorT3 waveforms and the numerical waveforms after the two-year inspiral are about $2 \times 10^3, 9 \times 10^1, 7 \times 10^{-1}, 7 \times 10^{-1}$ and 3×10^{-2} radians for 5.5, 10, 14, 18 and 22 PN, respectively. Therefore, we see that a 22 PN TaylorT3 waveform is required to get data analysis accuracies comparable to numerical waveform accuracy for System I.

The TaylorT3 approximant is not accurate in the case of System II as it goes up to the LSO ($v = 1/\sqrt{6}$). Even for System I, we find the dephase is a few orders of magnitude higher than that for TaylorT1. One also finds that the value of $F^{(\rm T3)}(t)$ becomes very large for $\theta(t) \geq 0.67$, and for System II one cannot find a $t_{\rm ref}$ consistent with the one derived for TaylorT2. The reason for this is again similar to the reason for the poor behavior of TaylorT4 as compared to TaylorT1. In the TaylorT3 approximation, one derives $v(t)$ as a series of t, i.e. θ, by iteratively inverting $t(v)$ in TaylorT2. $v(t)$ as a series of t can also be derived using $v(t) = \int (dv/dt')dt'$. Since the integrand of $v(t)$, dv/dt, has a pole at LSO, one will expect that $v(t)$ as a series of t does not converge well around LSO. Thus, functions of θ in TaylorT3, computed using $v(t)$ in a series of t, will not converge well.

IV. CONCLUSIONS

Using the 22 PN expression for flux, $\mathcal{F}(v)$, derived in Ref. [15], we calculated the TaylorT1, TaylorT2, TaylorT3, TaylorT4 and TaylorEt approximants up to 22 PN order for a test particle in a circular orbit around a Schwarzschild black hole. We evaluated the performance of the PN waveforms by calculating the gravitational wave phase predicted for two EMRI systems, System I ($m_1/m_2 = 10^{-4}$) and System II ($m_1/m_2 = 10^{-5}$) during two-year inspirals. System I (System II) corresponds to the early (late) inspiral phase of the eLISA frequency band. The phase predicted by PN waveforms is compared with the phase predicted by waveforms resulting from high-precision numerical solutions of the Teukolsky equation for the same inspirals. For accurate eLISA EMRI parameter estimation with these PN waveforms, we need the difference of the phases, the dephase, to be less than 10^{-2} radians [4].

We found that the dephase between the 22 PN waveforms and numerical waveforms after a two-year inspiral for System II is smaller than 10^{-2} and 10^{-3} radians for TaylorT1 and TaylorT2, respectively. Therefore, we expect that these 22 PN waveforms can be used to attain data analysis accuracies comparable to those provided by high-precision numerical waveforms for most of the parameter space of EMRIs. Moreover, for the early inspiral phase, 10 PN waveforms for TaylorT1 and TaylorT2 may be used for data analysis.

However, the dephase of TaylorT4, TaylorEt and TaylorT3 waveforms goes to values higher than 10^2 radians for System II. This suggests that these approximants cannot be used for data analysis of late inspirals. We note that our results reinforce investigations in Ref. [11] that TaylorEt and TaylorT3 are recommended not to be used for data analysis of comparable mass binaries.

For System I, we found that 14 PN or higher PN order waveforms are required for TaylorT4, TaylorEt and TaylorT3 to achieve comparable results in data analysis to using high-precision numerical waveforms even in the early inspiral phase. We also found that the reason the dephases of TaylorT4, TaylorEt and TaylorT3 waveforms are much larger than those of TaylorT1 and TaylorT2 may be related to the fact that $(dE/dv)^{-1}$ has a pole at the LSO. This suggests that when constructing templates for coalescing compact binaries, approximants avoiding the pole at the LSO arising from the energy function by factorizing it as in TaylorT1, or those introducing a new variable which cancels the pole, may perform better. We hope that these studies also provide insights to construct more efficient templates for coalescing compact binaries in the comparable mass case. Lastly, the analytical expressions for the

various approximants could also be useful for studies related to the ground-based detectors.

ACKNOWLEDGMENTS

V. V. and A. C. thank the Raman Research Institute for support during the Visiting Student Program, during which this work was initiated. R. F. is grateful for the support of the European Union FEDER funds, the Spanish Ministry of Economy and Competitiveness (Projects No. FPA2010-16495 and No. CSD2007-00042) and the Conselleria d'Economia Hisenda i Innovacio of the Govern de les Illes Balears.

[1] F. D. Ryan, Phys. Rev. D **52**, 5707 (1995).
[2] E. Berti, A. Buonanno, and C. M. Will, Classical Quantum Gravity **22**, S943 (2005).
[3] S. Drasco, Classical Quantum Gravity **23**, S769 (2006).
[4] J. Thornburg, arXiv:1102.2857.
[5] J. R. Gair, L. Barack, T. Creighton, C. Cutler, S. L. Larson, E. S. Phinney, and M. Vallisneri, Classical Quantum Gravity **21**, S1595 (2004).
[6] P. Amaro-Seoane *et al.*, arXiv:1201.3621.
[7] D. Merritt, T. Alexander, S. Mikkola, and C. M. Will, Phys. Rev. D **84**, 044024 (2011).
[8] L. Blanchet, Living Rev. Relativity **9**, 4 (2006).
[9] P. Ajith *et al.*, Phys. Rev. D **77**, 104017 (2008).
[10] A. Buonanno, Y. Pan, J. Baker, J. Centrella, B. Kelly, S. McWilliams, and J. van Meter, Phys. Rev. D **76**, 104049 (2007).
[11] A. Buonanno, B. R. Iyer, E. Ochsner, Y. Pan, and B. S. Sathyaprakash, Phys. Rev. D **80**, 084043 (2009).
[12] T. Damour, B. R. Iyer, and B. S. Sathyaprakash, Phys. Rev. D **63**, 044023 (2001).
[13] T. Damour, B. R. Iyer, and B. S. Sathyaprakash, Phys. Rev. D **66**, 027502 (2002).
[14] M. Sasaki and H. Tagoshi, Living Rev. Relativity **6**, 6 (2003).
[15] R. Fujita, Prog. Theor. Phys. **128**, 971 (2012).
[16] S. Teukolsky, Astrophys. J. **185**, 635 (1973).
[17] E. Poisson, A. Pound, and I. Vega, Living Rev. Relativity **14**, 7 (2011).
[18] L. Barack, Classical Quantum Gravity **26**, 213001 (2009).
[19] L. Barack and N. Sago, Phys. Rev. D **75**, 064021 (2007).
[20] L. M. Burko and G. Khanna, Phys. Rev. D **88**, 024002 (2013).
[21] N. Warburton, S. Akcay, L. Barack, J. R. Gair, and N. Sago, Phys. Rev. D **85**, 061501 (2012).
[22] R. Fujita and H. Tagoshi, Prog. Theor. Phys. **112**, 415 (2004).
[23] R. Fujita and H. Tagoshi, Prog. Theor. Phys. **113**, 1165 (2005).
[24] See Supplemental Material at http://link.aps.org/supplemental/10.1103/PhysRevD.88.024038 for the 22 PN expressions in MATHEMATICA formats.
[25] J. M. Bardeen, W. H. Press, and S. A. Teukolsky, Astrophys. J. **178**, 347 (1972).
[26] M. Boyle, D. A. Brown, L. E. Kidder, A. H. Mroué, H. P. Pfeiffer, M. A. Scheel, G. B. Cook, and S. A. Teukolsky, Phys. Rev. D **76**, 124038 (2007).
[27] A. Gopakumar, arXiv:0712.3236.
[28] S. Droz, D. J. Knapp, E. Poisson, and B. J. Owen, Phys. Rev. D **59**, 124016 (1999).
[29] T. Damour, B. R. Iyer, and B. S. Sathyaprakash, Phys. Rev. D **62**, 084036 (2000).
[30] R. Fujita, Prog. Theor. Phys. **127**, 583 (2012).
[31] R. Fujita and B. R. Iyer, Phys. Rev. D **82**, 044051 (2010).
[32] N. Yunes, A. Buonanno, S. A. Hughes, M. C. Miller, and Y. Pan, Phys. Rev. Lett. **104**, 091102 (2010).
[33] P. Amaro-Seoane, J. R. Gair, M. Freitag, M. C. Miller, I. Mandel, C. J. Cutler, and S. Babak, Classical Quantum Gravity **24**, R113 (2007).
[34] E. K. Porter, arXiv:0910.0373.
[35] T. Damour, B. R. Iyer, and B. S. Sathyaprakash, Phys. Rev. D **57**, 885 (1998).
[36] T. Damour, B. R. Iyer, and A. Nagar, Phys. Rev. D **79**, 064004 (2009).